Flexible generation of femtosecond cylindrical vector beams

(Invited Paper)

Yuquan Zhang (张聿全)[1,2], Xiujie Dou (豆秀婕)[1], Yong Yang (杨 勇)[2], Chen Xie (谢 辰)[3], Jing Bu (步 敬)[2,4,*], Changjun Min (闵长俊)[1], and Xiaocong Yuan (袁小聪)[1]

[1]*Nanophotonics Research Centre, Shenzhen University & Key Laboratory of Optoelectronic Devices and Systems of Ministry of Education and Guangdong Province, College of Optoelectronic Engineering, Shenzhen University, Shenzhen 518060, China*

[2]*Key Laboratory of Optical Information Science and Technology of the Education Ministry of China, Institute of Modern Optics, Nankai University, Tianjin 300071, China*

[3]*Ultrafast Laser Laboratory, Key Laboratory of Opto-electronic Information Technical Science of Ministry of Education, College of Precision Instruments and Opto-electronics Engineering, Tianjin University, Tianjin 300072, China*

[4]*College of Mathematics and Statistics, Shenzhen University, Shenzhen 518060, China*

**Corresponding author: jingbu@szu.edu.cn*

Received November 12, 2016; accepted January 20, 2017; posted online February 14, 2017

Femtosecond (fs) cylindrical vector beams (CVBs) have found use in many applications in recent years. However, the existing rigid generation methods seriously limit its development. Here, we propose a flexible method for generating fs-CVBs with arbitrary polarization order by employing half wave plates and vortex retarders. The polarization state, autocorrelation width, pulse width, and spectrum features of the input and generated CVB pulses are measured and compared. The results verify that the generated CVBs remain in the fs regime with no appreciable temporal distortion, and the energy conversion efficiency can reach as high as 96.5%, even for a third-order beam. As a flexible way to generate fs-CVBs, this method will have great significance for many applications.

OCIS codes: 260.5430, 320.2250.
doi: 10.3788/COL201715.030007.

Cylindrical vector beams (CVBs) have gained much interest because of their unique polarization properties[1,2]. They have been widely applied and play an important role in many optical fields, such as optical trapping[3–5], optical communications[6,7], laser fabrication[8], imaging[9,10], and sensing[11]. In recent years, CVBs in the femtosecond (fs) field have been widely applied in processing, optical limiting, *etc.*[12–15], as a result of advantages that include ultrahigh peak power and ultrafast pulses. Generation of fs-CVBs has great importance for many fields of research and applications[16–21]. For the generation of common CVBs, many methods have been proposed, including inserting laser intracavity devices[22–24] or applying devices with spatially variant polarization properties[25–28], such as Q-plate, axial birefringence, and dichroism. However, in these methods, high flexibility and energy efficiency are usually mutually exclusive, and a pulse width broadening is inevitable. Meanwhile, the processing difficulty sharply increases with higher polarization orders of CVBs, as polarization exhibits more complex spatial inhomogeneous distribution with increased orders[24].

In this work, fs-CVBs with an arbitrary order were flexibly generated with high energy efficiency and pure polarization properties from a linearly polarized beam by employing combined vortex retarders (VRs, Thorlabs Inc.) and half wave ($1/2\lambda$) plates. Higher-order fs-CVBs, with odd and even, negative and positive orders, were experimentally generated by cascading VRs and $1/2\lambda$ plates. The polarization, autocorrelation width, pulse width, and spectrum features of the original and generated pulse were measured and detected. The results verified that the fs-CVBs have a perfect polarization quality and remain in the fs regime with no appreciable temporal distortion. In addition, the energy conversion efficiency is higher than 96.5% for order of 3. This method is therefore verified as a flexible way to generate CVBs with arbitrary orders, and it will be a significant method for fs-CVBs' research in the future.

The schematic of the fs-CVBs' generation setup is shown in Fig. 1, which shows the generation of a negative first-order ($m = -1$) fs-CVB by applying a VR and two $1/2\lambda$ plates. A mode-locked Ti:sapphire laser with a central wavelength of 800 nm was used as the source, with an original laser source pulse width of ~37 fs. The laser beam is first expanded and collimated in front of the polarizer (P_1) to obtain a linearly polarized beam before contacting the VR. The VR is a specially designed $1/2\lambda$ plate with a fast axis rotating continuously around the center (as shown in Fig. 1) with ultrahigh transmittance (>99%), whose Jones matrix can be derived as

$$\mathbf{M}_1 = \begin{bmatrix} \cos\varphi & -\sin\varphi \\ \sin\varphi & \cos\varphi \end{bmatrix}, \tag{1}$$

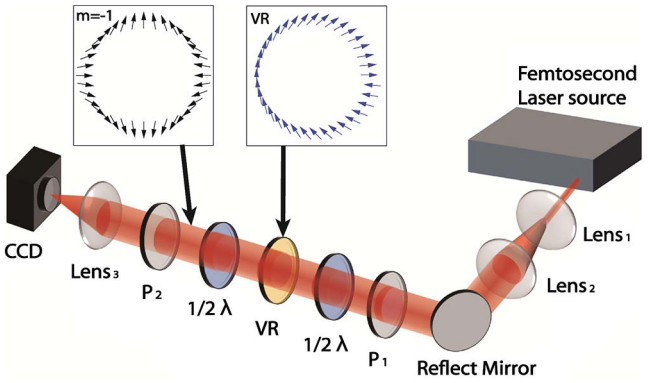

Fig. 1. Configuration of generation of negative first-order fs pulsed CVB. Any other orders can be generated by inserting the VR and $1/2\lambda$ plates. The blue arrows in the subgraph are the direction of the VR's fast axis, and the black ones depict polarization of generated CVBs.

where ϕ is the azimuthal angle. For a $1/2\lambda$ plate, the Jones matrix is

$$\mathbf{H}_0 = \begin{bmatrix} \cos 2\phi & \sin 2\phi \\ \sin 2\phi & -\cos 2\phi \end{bmatrix}, \tag{2}$$

where ϕ is the angle of the fast axis of the $1/2\lambda$ plate with the x axis. Then, a complex ordered $\mathbf{M}_m$ (m is a positive integer defining the polarization order of the CVB, with polarization rotations of $m * 2\pi$ along the clockwise circle direction) can be obtained by coaxial combination of the VRs and $1/2\lambda$ plates as follows:

$$\mathbf{M}_m = \mathbf{M}_{m-1}\mathbf{H}_0\mathbf{M}_1, \tag{3}$$

$$\mathbf{M}_{-m} = \mathbf{H}_0\mathbf{M}_m\mathbf{H}_0. \tag{4}$$

Spontaneously, an incident linearly polarized beam can be converted into an mth-order CVB using the relationship $\mathbf{E}_m = \mathbf{M}_m\mathbf{E}_l$, where the Jones matrices of the linearly polarized beam $\mathbf{E}_l$ and the mth-ordered CVB $\mathbf{E}_m$ are

$$\mathbf{E}_l = \begin{bmatrix} \cos\theta \\ \sin\theta \end{bmatrix}, \tag{5}$$

$$\mathbf{E}_m = \begin{bmatrix} \cos(m\varphi + \varphi_0) \\ \sin(m\varphi + \varphi_0) \end{bmatrix}, \tag{6}$$

where θ is the orientation of the incident linear polarization with respect to the x axis, and φ_0 is the inner polarization rotation of the CVB.

Consequently, an incident linearly polarized beam that goes through a converter with a Jones matrix of $\mathbf{M}_m$, by a combination of the VRs and $1/2\lambda$ plates, will be converted into an mth-order cylindrically symmetric polarized beam. As the fast axis of the VR exhibits asymmetrical spatial inhomogeneous distribution, CVBs with different polarization states can be obtained by rotating their orientation consecutively, from radially to azimuthally polarized, at each point. Polarization of the generated fs-CVBs can be directly observed using CCD cameras, after passing through a polarizer (P_2) and a neutral density filter.

CVBs with higher orders are slightly more complicated to generate, where the VR and $1/2\lambda$ plates are used as the basic unit. An $(m+n)$th-order CVB will be generated after adding n groups of $1/2\lambda$ plates and VRs from the derivation of Eq. (3) after the already mth-order CVB. For instance, a third-order CVB is generated by inserting a $1/2\lambda$ plate and a VR after the second-order CVB. Furthermore, the reversed process of reducing the order of CVBs also has great potential applications where demodulating signals are needed, such as optical communications. To generate lower-order CVBs, it is still convenient to obtain m–nth-order CVBs using incident mth-order CVBs passing through n numbers of VRs. It is noteworthy that the orientation of VRs should be accurately homocentric and regulated to be directed parallel to each other. In addition, the polarized state of output CVBs can be adjusted to an orthogonal polarization by rotating the polarized direction of the incident linearly polarized beam. For negative mth-order CVBs, two additional $1/2\lambda$ plates are placed in front of the plates and after the mth-order CVB, respectively, as shown in Eq. (4). For instance, the negative first-order output fs-CVB is generated by adding a $1/2\lambda$ plate in front of and after the VR, as shown in Fig. 1.

To verify the capability of generating arbitrary-order fs-CVBs, different-order CVBs were realized by a combination of VRs and $1/2\lambda$ plates. All of the intensity distributions of the CVBs were generally similar and donut-shaped, but with different radius ratios. Polarization features were detected by inserting a polarizer after the generated CVBs. When passing through polarizer P_2, petal-shaped patterns were received by the CCD. The petal numbers N ($N = 2|m|$, m is the order of the CVB) after a polarizer denote the absolute value of the CVB order. However, the patterns of negative and positive CVBs with the same order after passing through polarizer P_2 are the same; thus, further detection should be applied to distinguish the $\pm m$th-order fs-CVBs, such as exciting surface plasmons on a metal surface[4,29] or employing vortex phase elements[30]. Figure 2 depicts the polarization of the generated 800 nm fs-CVBs with different orders, where (a)–(d) are the polarization distributions of the first, second, third, and fourth-order fs pulsed CVBs, (e)–(h) show the intensity distributions of the CVBs, which are generally similar and donut-shaped but with different radius ratios, and (i)–(l) are the petal intensity distributions of the fs pulsed CVBs after the second polarizer (P_2 in Fig. 1), as captured by a CCD camera. Figure 3 shows the corresponding petal intensity distributions of the third-order CVB after polarizer P_2 with different polarization angles (θ). The shape invariance of each lobe proves the highly polarized quality of the generated CVBs.

As fundamental physical quantities of the pulsed laser, the measured autocorrelation widths (FWHM) of the fs-CVBs with different orders are presented in Table 1. Variation occurs with inserted wave plates in the optical path, and slight pulse broadening inevitably appears when

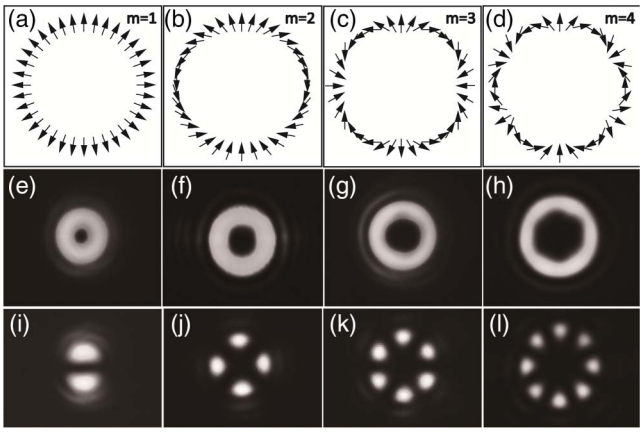

Fig. 2. Detection of output fs pulsed CVBs. (a)–(d) polarization distribution of the first, second, third, and fourth-order fs pulsed CVBs, (e)–(h) the intensity distribution of CVBs, which are generally similar and donut-shaped but with different radius ratios, (i)–(l) petal intensity distribution of CVBs after a polarizer.

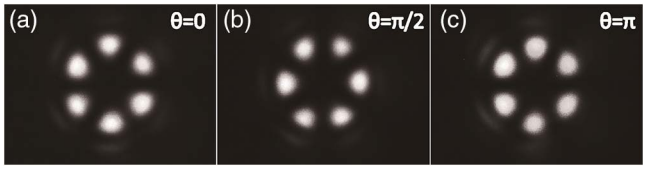

Fig. 3. Petal intensity distribution after the polarizer with different polarization angles (θ).

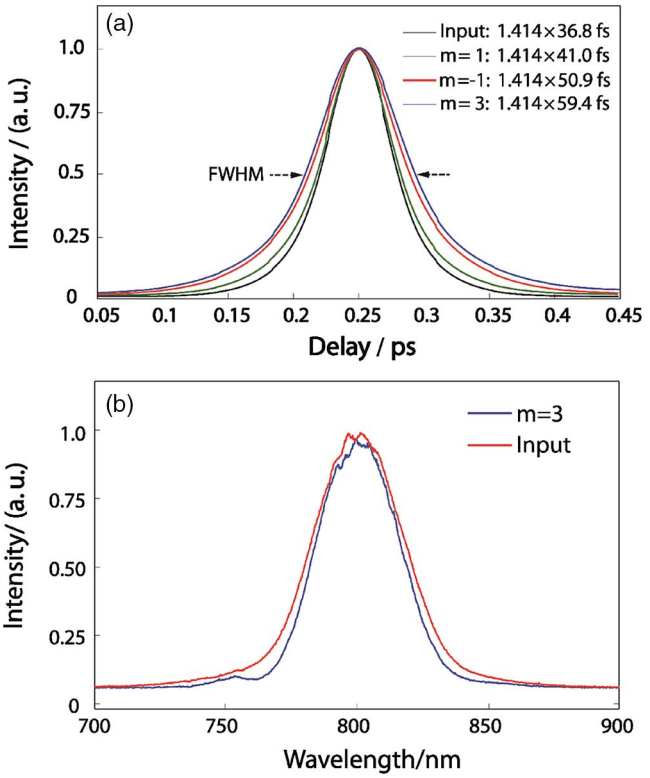

Fig. 4. (a) Time domain comparison and (b) optical spectrum of the input beam and generated CVBs. The pulse is stretched by several fs for each optical component, and it only shows a slight difference in the spectral profile.

the laser pulses pass through the dispersive components. The measured energy of each sampled beam is presented, and the efficiencies can reach as high as 96.5%, even for the third-order CVB. Figure 4(a) shows a comparison of the original beam with the generated sample beams in the temporal domain. The pulse width of the laser source is ~37 fs (assuming a Gaussian shape), and the pulse width broadened by several fs (<9 fs) for a single wave plate set (*i.e.*, a $1/2\lambda$ plate and a VR). Thus, both high flexibility and high efficiency can be maintained in our scheme. The spectra of the original beam and the third-order CVB with a central wavelength of 800 nm were further measured, as shown in Fig. 4(b). The spectral profile of the third-order fs-CVB is very close to that of the input pulse, with only minor differences. These results indicate that the fs-CVBs can maintain fs pulse durations, even with the insertion of three wave plate sets in our scheme, with negligible spectral distortions.

In conclusion, we demonstrate a flexible method for the generation of CVBs in the fs regime with high pure polarization properties and energy transmission efficiency. A linearly polarized beam can be converted into arbitrary-order CVBs by combining VRs and $1/2\lambda$ plates based on the Jones matrix derivation. The polarization is detected by passing through a polarizer to form petal-shaped patterns, and the invariance of the lobes proves the highly polarized quality of generated CVBs. Fundamental physical quantities of the pulsed laser, including the variation of the autocorrelation width, energy intensity, pulse width, and spectra, are further measured experimentally. The results indicate that the generated CVBs remain in the fs regime with insignificant spectral distortion, and energy efficiency can reach as high as 96.5%, even for the third-order CVB. This method provides a flexible way to generate arbitrary-order CVBs, and it has great potential for various applications.

Table 1. Experimental Pulse Statistics of the Original and Generated Beams

	Autocorrelation width/fs	Power/mW
Original beam	52	434.5
1-order CVB	58	430.6
−1-order CVB	72	425.9
3-order CVB	84	419.7

This work was supported by the National Natural Science Foundation of China (Nos. 61138003, 61427819, 61422506, 61605117, and 61605142), the Science and Technology Innovation Commission of Shenzhen (Nos. KQCS2015032416183980, KQCS201532416183981, and JCYJ20140418091413543), and the start-up funding

at Shenzhen University. X. Y. appreciates the support given by the Leading Talents of Guangdong Province Program (No. 00201505), and the Natural Science Foundation of Guangdong Province (No. 2016A030312010). Y. Z. appreciates the support of Natural Science Foundation of Guangdong Province (No. 2016A030310063), the Project 2016032 supported by the SZU R/D Fund, and the Open Fund of the Key Laboratory of Optical Information Science & Technology (Nankai University). The authors thank Dr. Haochen Tian and Dr. Xiaoyu Weng for their help in the experiments.

References

1. Q. Zhan, Adv. Opt. Photon. **1**, 1 (2009).
2. K. S. Youngworth and T. G. Brown, Opt. Express **7**, 77 (2000).
3. L. Huang, H. L. Guo, J. F. Li, L. Ling, B. H. Feng, and Z. Y. Li, Opt. Lett. **37**, 1694 (2012).
4. C. J. Min, Z. Shen, J. F. Shen, Y. Q. Zhang, H. Fang, G. H. Yuan, L. P. Du, S. W. Zhu, T. Lei, and X. C. Yuan, Nat. Comm. **4**, 2891 (2013).
5. S. Roy, K. Ushakova, Q. van den Berg, S. F. Pereira, and H. P. Urbach, Phys. Rev. Lett. **114**, 103903 (2015).
6. Y. F. Zhao and J. Wang, Opt. Lett. **40**, 4843 (2015).
7. G. Milione, T. A. Nguyen, J. Leach, D. A. Nolan, and R. R. Alfano, Opt. Lett. **40**, 4887 (2015).
8. B. H. Jia, H. Kang, J. F. Li, and M. Gu, Opt. Lett. **34**, 1918 (2009).
9. G. Bautista, M. J. Huttunen, J. Mäkitalo, J. M. Kontio, J. Simonen, and M. Kauranen, Nano Lett. **12**, 3207 (2012).
10. K. Yuichi and S. Sato, Opt. Express **23**, 2076 (2015).
11. C. L. Zhang, R. Wang, C. J. Min, S. W. Zhu, and X. C. Yuan, Appl. Phys. Lett. **102**, 011114 (2013).
12. G. D. Tsibidis, E. Skoulas, and E. Stratakis, Opt. Lett. **40**, 5172 (2015).
13. O. J. Allegre, W. Perrie, S. P. Edwardson, G. Dearden, and K. G. Watkins, J. Opt. **14**, 085601 (2012).
14. J. L. Wu, B. Gu, N. Sheng, D. H. Liu, and Y. P. Cui, Appl. Phys. Lett. **105**, 171113 (2014).
15. K. K. Anoop, A. Rubano, R. Fittipaldi, X. Wang, D. Paparo, A. Vecchione, L. Marrucci, R. Bruzzese, and S. Amoruso, Appl. Phys. Lett. **104**, 241604 (2014).
16. K. J. Moh, X.-C. Yuan, J. Bu, D. K. Y. Low, and R. E. Burge, Appl. Phys. Lett. **89**, 251114 (2006).
17. G. Liu, Y. Yang, Y. He, X. Zheng, and Z. Luo, Acta Opt. Sin. **35**, 0526001 (2015).
18. T. Duan, P. Jin, and C. Li, Chin. Opt. Lett. **9**, s10602 (2011).
19. J. L. Qi, W. C. Sun, J. L. Liao, Y. M. Nie, X. F. Wang, J. Zhang, X. S. Liu, H. Jia, M. Lu, S. R. Chen, J. Liu, J. K. Yang, J. C. Tan, and X. J. Li, Opt. Eng. **52**, 024201 (2013).
20. Z. Fang, Y. Yao, K. Xia, and J. Li, Chin. Opt. Lett. **13**, 031405 (2015).
21. K. J. Moh, X. C. Yuan, J. Bu, R. E. Burge, and B. Z. Gao, Appl. Opt. **46**, 7544 (2007).
22. K. Yonezawa, Y. Kozawa, and S. Sato, Opt. Lett. **31**, 2151 (2006).
23. G. Machavariani, Y. Lumer, I. Moshe, A. Meir, S. Jackel, and N. Davidson, Appl. Opt. **46**, 3304 (2007).
24. X. L. Wang, J. Ding, W. J. Ni, C. S. Guo, and H. T. Wang, Opt. Lett. **32**, 3549 (2007).
25. Q. Zhan and J. R. Leger, Appl. Opt. **41**, 4630 (2002).
26. L. Marrucci, C. Manzo, and D. Paparo, Phys. Rev. Lett. **96**, 163905 (2006).
27. C. Rotschild, S. Zommer, S. Moed, O. Hershcovitz, and S. G. Lipson, Appl. Opt. **43**, 2397 (2004).
28. G. Machavariani, Y. Lumer, I. Moshe, A. Meir, and S. Jackel, Opt. Commun **281**, 732 (2008).
29. Y. Zhang, J. Wang, J. Shen, Z. Man, W. Shi, C. Min, G. Yuan, S. Zhu, H. P. Urbach, and X. Yuan, Nano letters **14**, 6430 (2014).
30. S. N. Khonina, D. A. Savelyev, and N. L. Kazanskiy, Opt. Express **23**, 17845 (2015).